

Numerical and Experimental Study of Residual Stress Measurement and Thickness Distribution of T-shape Steel Tube Produced by Tube Hydroforming

Javad Shahbazi Karami^{1*}, Gholamhasan Payganeh¹, Mohsen Khodsetan²

¹Faculty of Mechanical Engineering, Shahid Rajaee Teacher Training University, Tehran, Iran

²School of Mechanical Engineering, College of Engineering, University of Tehran, Tehran, Iran

*Email of Corresponding author: Shahbazi.mech@gmail.com

Received: April 14, 2019; Accepted: January 2, 2020

Abstract

Tube hydroforming (THF) process is used to produce the complex components from the initial cylindrical tubes. In this paper, T-shape component was formed using a tube hydroforming machine and the residual stresses of hydroformed tube was determined by hole drilling method. Subsequently, the thickness distribution and residual stresses of final tube were investigated using experimental and finite element (FE) methods. The results represented the top of the protrusion has the minimum thickness, whereas the maximum thickness appears in the bottom zone of T-shape tube. The FE results showed that the maximum principal stress in the middle part of piece has own maximum value while the maximum value of minimum principal stress is located in the top of protrusion and the fillet transition region of the protrusion. It is found that the value of residual stress, protrusion height and thickness distribution in simulated results were in good agreement with the experimental results.

Keywords

T-shaped Tube Hydroforming, Finite Element, Residual Stress, Hole Drilling

1. Introduction

Tube hydroforming is an advance metal forming process based on high fluid pressure to producing the hollow complex components [1]. The first invention contained apparatus for making T-shape components published in the USA in 1940 [2]. Several works including the numerical, analytical and experimental studies have been done on the effect of different parameters of THF technique. The effect of friction coefficient and lubrication on the thickness distribution and height of protrusion was investigated by Limb et al. [3]. Woo [4] investigated the bursting conditions of thin-walled cylindrical component by an analytical solution. Thiruvarudchelvan et al. [5] studied the theoretical and experimental characteristics of tube bulging technique. Powell and Avitzur [6] calculated the internal pressure as function of geometry and material properties with an upper bound solution. Multi-branches tubes such as seamless T-shape, Y-shape and X-shape are the common components that are used in automotive, aerospace, oil and gas industries [1]. Accurate control of the of the THF process parameters such as internal pressure, axial feed force, counter punch force and calibrating pressure are problems of THF process. Researchers and industrialists have done several studies to solve drawbacks of the multi-branches hydroforming technique. Ogura and Ueda [7] formed T-shapes low and medium carbon steel parts by liquid bulge forming. Limb et al. [8] evaluated achievable height of protrusion in the forming of T-shaped tubular components by

different material such as aluminum, low carbon steel, brass and copper. Hwang and Chang [9] designed and developed a hydroforming machine for producing the T-branch protrusion parts with counter punch. Hwang and Lin [10] presented finite element (FE) model for simulation of the THF process with axial feeding and internal pressure. They modeled this process by using DEFORM 3D finite element code. Crapps et al. [11] carried out experimental and parametric FE analysis to evaluate the characteristics of bucking system and pressure profiles that related to final part. A virtual database assisted fuzzy control system to obtain optimal loading path in T-branch hydroforming operation developed by Manabe et al. [12]. Loh-Mousavi et al. [13] improved the formability of T-shape components by converting the internal pressure to pulsating pressures. They used FE simulation to examine the formability improvement mechanisms and thinning behavior. Ray and Mac Donald [14] simulated the T- and X-branch hydroforming technique to investigation of maximum attainable branch height and thickness distribution of final parts. They used LS-DYNA3D explicit FE code and validated the FE results via experimental results that performed on the initial copper tubes. Despite the many researches done on the different approach of T-shape hydroforming process, no works have been investigated to measure the residual stress of hydroformed T-branch. On the other hand, residual stresses are affected on the fracture, wear, fatigue, dimensional instability, stress corrosion and distortion [15]. There are many methods to measure residual stresses such as neutron powder diffraction, x-ray diffraction, hole drilling and layer removal sectioning. Among a mentioned methods, the hole drilling is a easily, semi-destructive and reliably experimental method that widely used to obtain experimental residual stresses in structures and materials [16, 17]. This method is presented by Van Crombrugge and Kelsey [18] to measure the strain at incremental depth to record the residual stresses. The procedure of hole drilling technique has been standardized and this procedure described in ASTM Standard Procedure E837 for various metallic plates [19].

It is accordingly an object of the present study to investigation of residual stresses at final hydroformed T-branch. In this paper, experimental study and FE simulation of T-branch tube hydroforming is performed. Also, distribution of thickness and residual stresses are investigated. By comparing the experimental results with the simulated results, the validity of the thickness distribution and residual stresses confirmed.

2. THF process of T-shape component and experimental procedure

Schematic of T-shape hydroforming process exhibits in Figure 1. Step (i): The initial tube at the starting of process is put into the die cavity. Step (ii): Die is closed and tube is filled with liquid. Step (iii): The punches moves to impose axial feed force and pressure is added to form the T-shape tube. Also counter punch is pushed on the top of the branch to avoid rupture of final tube. Step (iv): T-shape tube formed and the ejection of T-branch part is done.

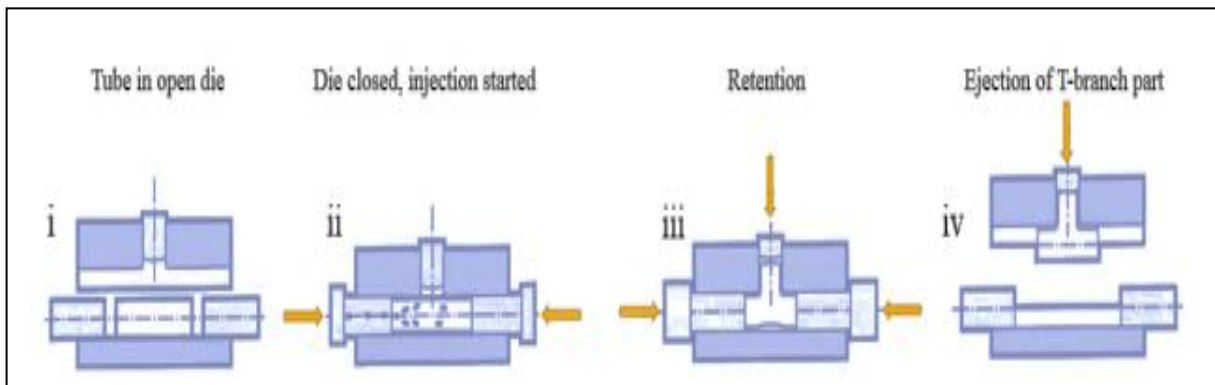


Figure1. Schematic of T-shape hydroforming process

The Tube of A106 GR.B steel with 120 mm length, 60 mm diameter and 5 mm thickness was used. According to the FE results, experimental work has been done in the TOOS PAVAND factory. The experimental set-up and hydroformed tube are shown in Figure 2.

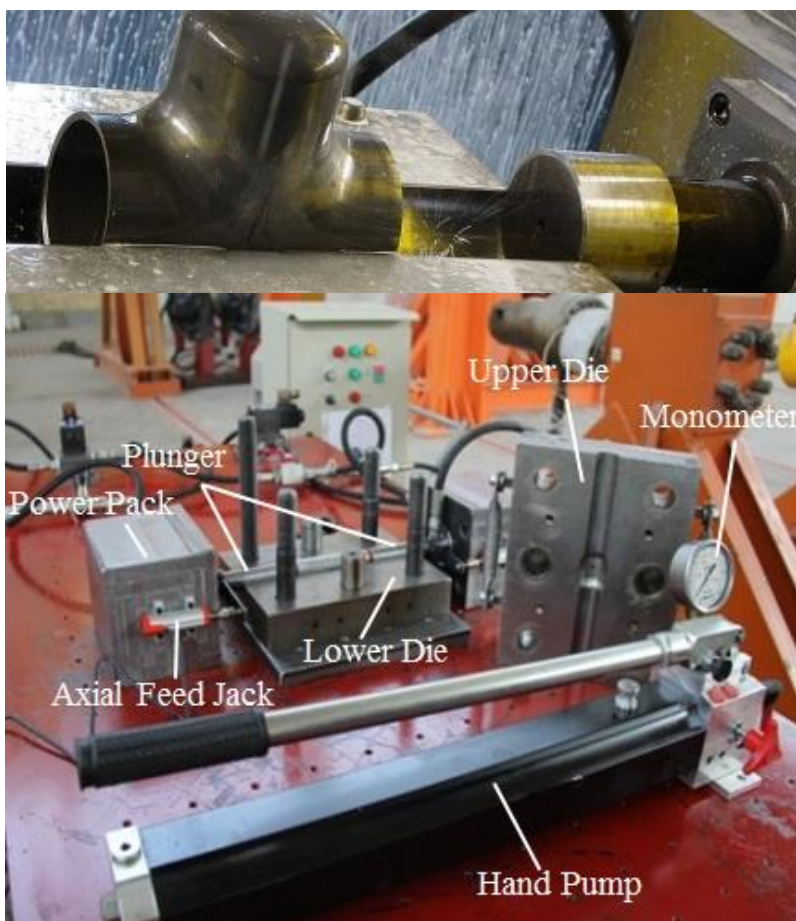


Figure2. Hydroforming Machine in ShahidRajae University

Figure 3 shows the strain gauge rosettes attached to the surface of the protrusion of T-shape specimen on which the residual stresses are determined. A small hole is accurately drilled with using a precise milling guide as shown in Figure 3(a). Three elements TML make FRS-3-17 strain

gauge rosette were used. The hole diameter of strain gauge rosette was 3.5 mm. The changes of strain are measured by strain gauge rosettes when the hole is drilled. Then the residual stresses was calculated by relative equation.

The principle strain was obtained from hole drilling technique and then residual stress was calculated according to Equations (1), (2) and (3) [20].

$$\sigma_{\max} = \frac{\varepsilon_1 + \varepsilon_3}{4A} - \frac{1}{4B} \sqrt{(\varepsilon_3 - \varepsilon_1)^2 + (\varepsilon_3 + \varepsilon_1 - 2\varepsilon_2)^2} \quad (1)$$

$$\sigma_{\min} = \frac{\varepsilon_1 + \varepsilon_3}{4A} + \frac{1}{4B} \sqrt{(\varepsilon_3 - \varepsilon_1)^2 + (\varepsilon_3 + \varepsilon_1 - 2\varepsilon_2)^2} \quad (2)$$

$$\tan 2\alpha = \frac{\varepsilon_1 - 2\varepsilon_2 + \varepsilon_3}{\varepsilon_3 - \varepsilon_1} \quad (3)$$

Where σ_{\max} and σ_{\min} are maximum and minimum principle residual stresses, ε_1 , ε_2 and ε_3 are the strains reading of strain gauges, \bar{A} and \bar{B} are the calibration coefficients and α is the angle between the location of gauge 1 and direction of maximum principle residual stress, σ_{\max} . The value of calibration coefficients depends on the strain gauge rosette geometry, the hole diameter, the hole depth, material properties and applied load [20, 21].

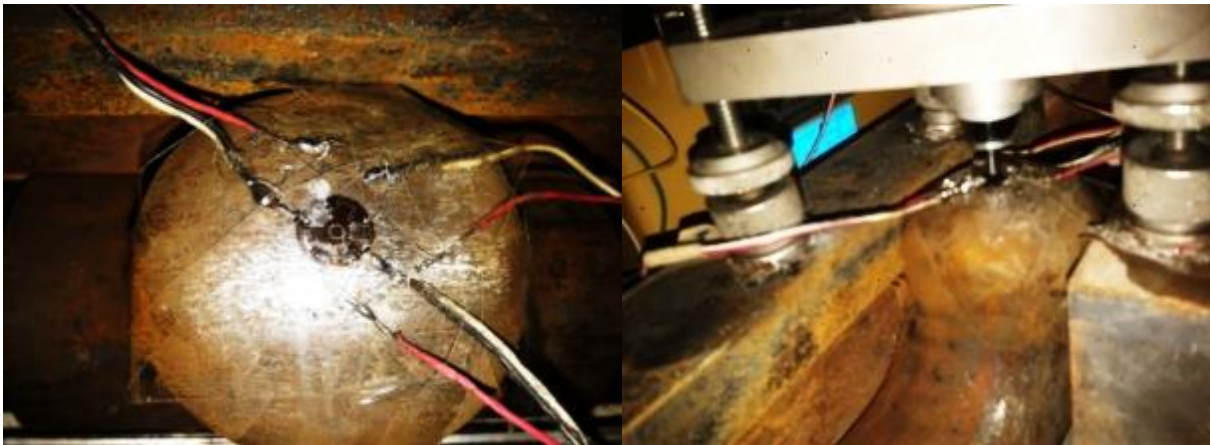


Figure3. Experimental Test of Residual Stress Measurement

3. FE modelling

3.1. FE procedure

The simulation of T-shape tube hydroforming is done using commercial FEM code (Abaqus/Explicit). The FE simulations performed with 3D model. To direct comparison of experimental and simulation results, the mechanical properties and geometrical dimensions of samples were the same as the experiment. The flow stress of material in the simulation model was

obtained from ASTM A106 Grade B. The workpiece was meshed using 7500C3D8R solid elements. The arbitrary Lagrangian-Eulerian (ALE) adaptive meshing was used for automatically remeshing the distorted elements during the T-shape tube hydroforming simulation. The Coulomb friction and penalty method was assumed between surfaces of the tube and die interactions. The hydroforming die and counter punch model were considered analytical rigid parts.

Figure 4 shows the stress-strain curves obtained at room temperature from the initial sample. The flow stress of material in the simulation model was obtained from the tensile test. The flow stress of the tube material was obtained by a tensile test and is expressed by a power law of its equivalent strain, i.e., $\bar{\sigma} = K\bar{\varepsilon}^n$ where $K = 800\text{MPa}$ is the strength coefficient and $n = 0.3$ is the strain hardening exponent. For description of material behavior in the simulation process equation 4 was used, where σ is flow stress and ε is the effective strain.

$$\sigma = 800\varepsilon^{0.3} \tag{4}$$

The values of process parameters and experimental A106 steel properties are shown in Table 1. In this study, three paths were selected to investigate the thickness distribution and residual stresses that observable in Figure 5.

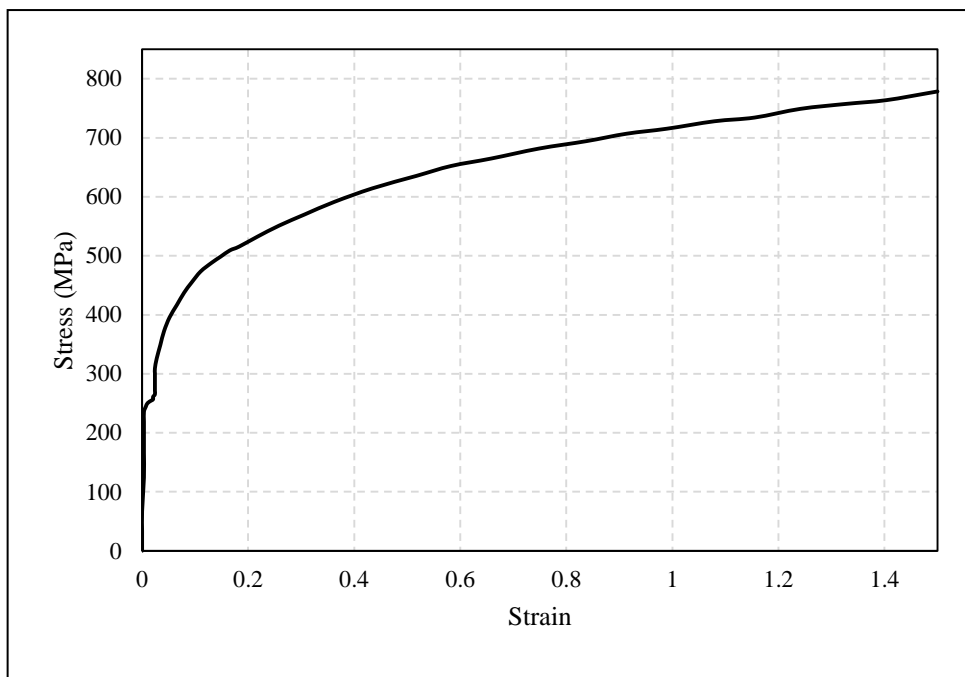


Figure4. Stress-Strain Curve of initial sample

Table1. The experimental A106 steel physical properties and process parameters

Parameter	Value
Young's modulus (E)	210 GPa
Poisson's ration (ν)	0.3
Density (ρ)	7850 Kg/m ³
Tube length (l)	0.216 m
Initial thickness (t_i)	0.005 m
Tube diameter (D_o)	0.060 m
Friction coefficient (μ)	0.1

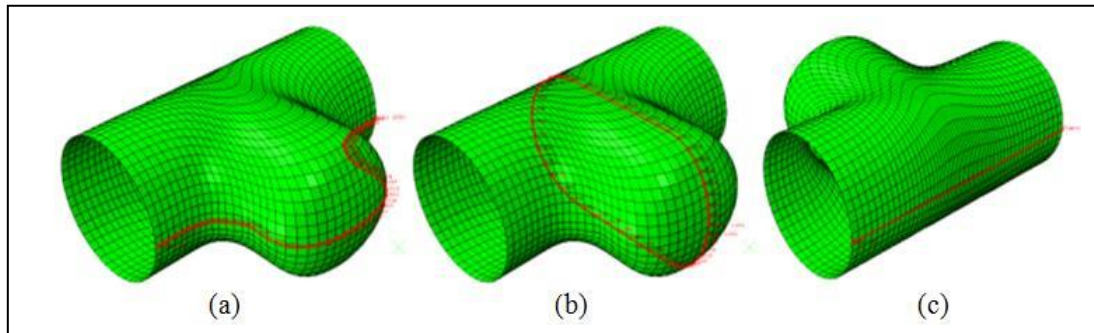


Figure5. (a) The upper transition path of the protrusion, (b) The lower surface of T-shape tube path and (c) The transition annular path of the protrusion

3.2. Thickness distribution

After hydroforming process, the thickness of T-branch is changed due to the high pressure fluid, intense deformation and flow of material into the die as a result of plastic deformation. Figure6 displays the thickness contours of T-branch tube obtained by FE simulation. The thickened regimes are located in the middle of lower part of T-shape tube and the fillet transition region of the protrusion. The maximum thickness reduction is occurred at top of the protrusion with the value of 3.955 mm. In THF process, the branch forming and flow of tube materials is caused to reduce the thickness of branch wall. The minimum tube wall thickness reduction at the middle of lower part of T-shape part is 6.865 mm.

Figure7 a-c shows the upper transition path of the protrusion, the bottom surface of T-shape tube path and the transition annular path of the protrusion to investigate the thickness distribution in different regions. As can be seen, the curves of thickness distribution are symmetric due to the symmetry of the considered paths.

According to the forming time, the largest reduction is occurred in the calibration step. The thickness of the regions in contact with the die surfaces has not significantly changed and the friction force has more effect on the thickness thinning.

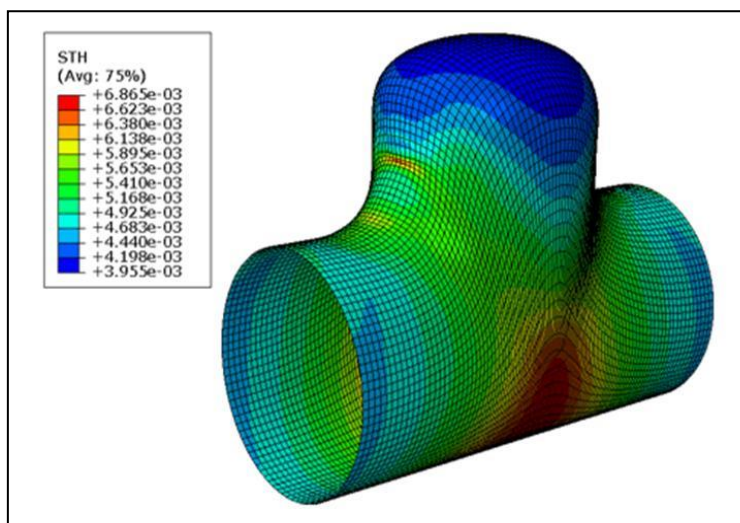


Figure6.Thickness contours of hydroformed T-branch tube

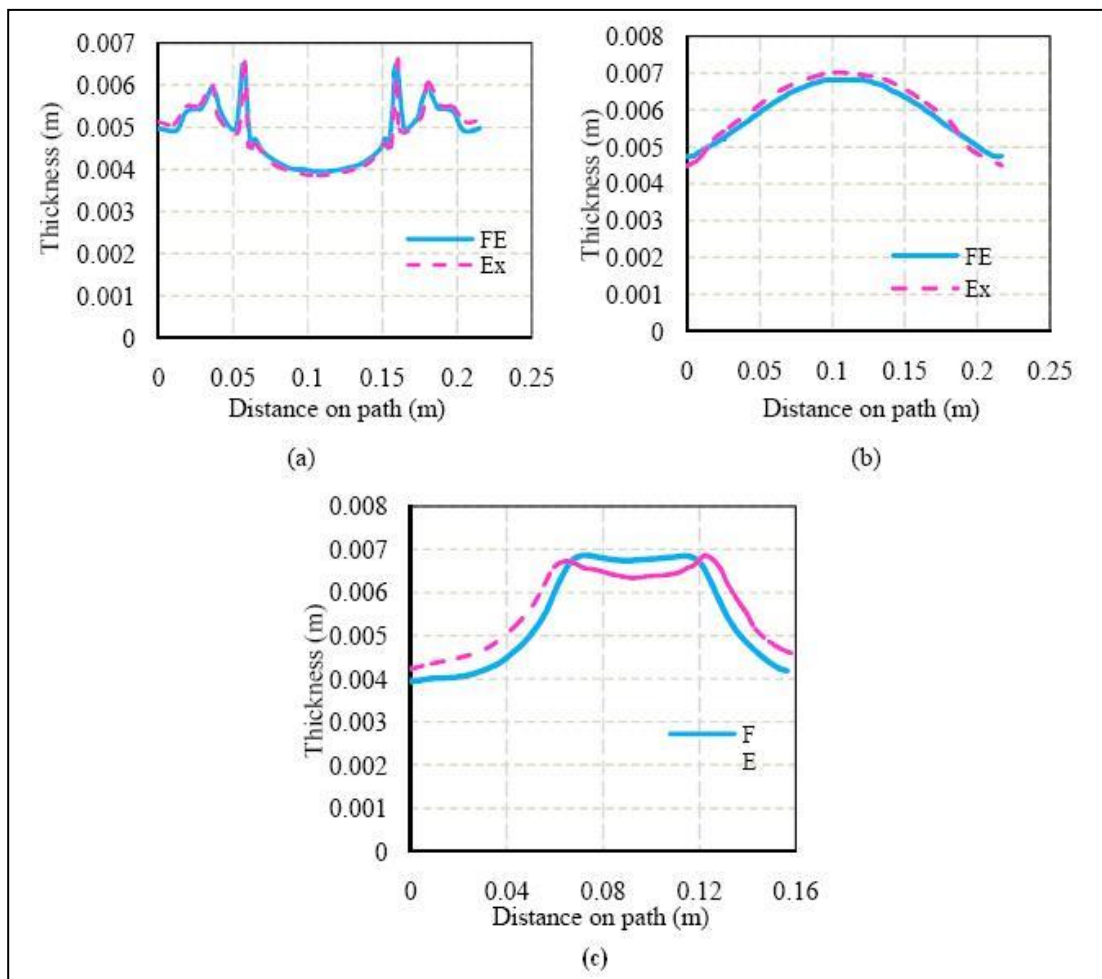


Figure7.Thickness distribution along the (a) the upper transition path of the protrusion, (b) the lower part of T-shape tube path and (c) the transition annular path of the protrusion

3.3. Stress distribution

Figure 8 represents the maximum and minimum principal stress contours of T-branch tube obtained by FE simulation. It can be seen that the maximum stress region is around the formed branch. Due to the high pressure required for deformation of protrusion, the protrusion area are under the high stresses. The maximum principal stress in the middle of piece has its own maximum value. The axial feed and flow of the material in the fillet of the die for forming the protrusion are caused the high stresses in the area. The maximum value of minimum principal stress is located in the top of protrusion and the fillet transition region of the protrusion. The stress distribution is in good agreement with the distribution of thickness thinning because the intense deformation is occurred in these regions. In the forming of protrusion, tensile stresses are applied to the tube wall in branch zone. The main result of tensile stresses is necking that this phenomenon occurs in the protrusion wall.

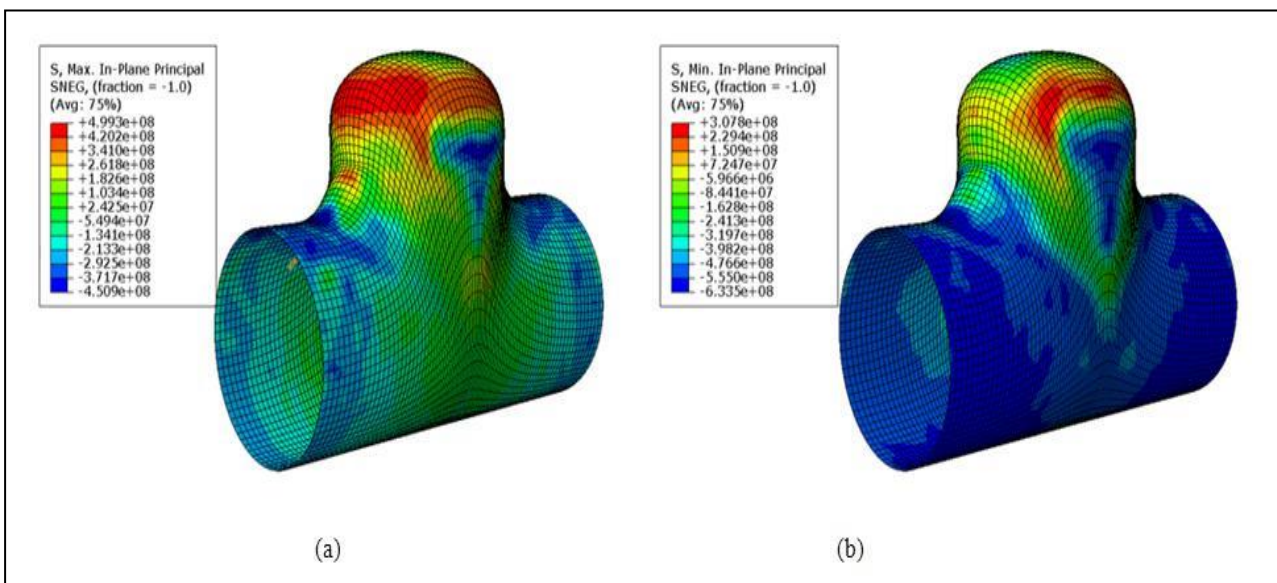


Figure8. The contours of the (a) maximum and (b) minimum principal stress

Figure 9-11 shows changes of the maximum and minimum principal stress along the upper transition path of the protrusion, the bottom surface of T-shape tube path and the transition annular path of the protrusion. It can be seen that the compressive and tensile stresses was observable in different zone of formed components. The tensile stress is appeared due to the forming of branch. The compressive stress is appeared because of the axil feed force. The compressive and tensile stresses are determined the thickness distribution of final components. The tensile stress is caused to thin the thickness of tube wall. On the other hand, the compressive stress is caused to thicken the tube wall.

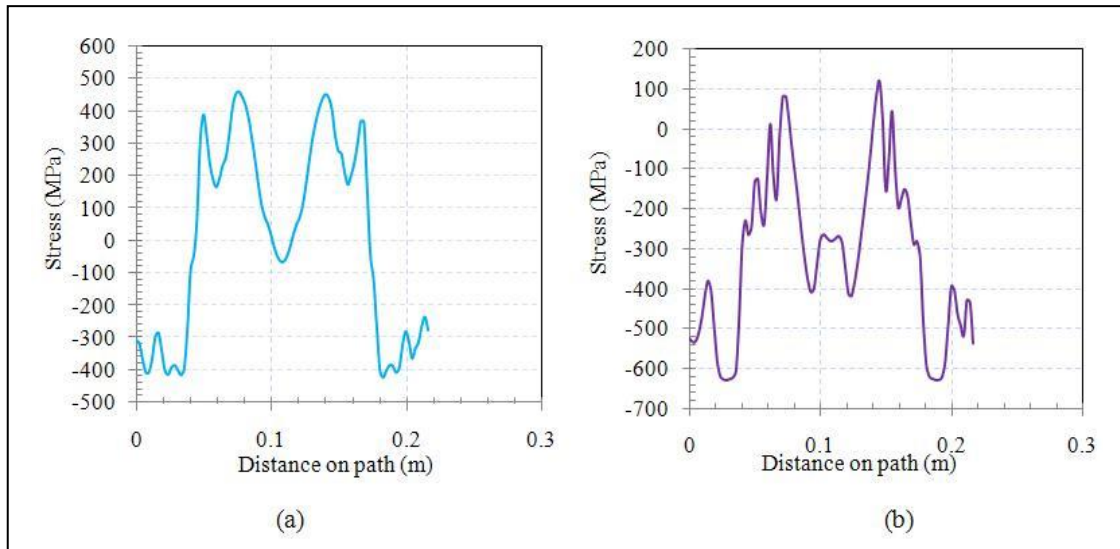


Figure9. Changes diagram of the (a) maximum and (b) minimum principal stress at the upper transition path of protrusion

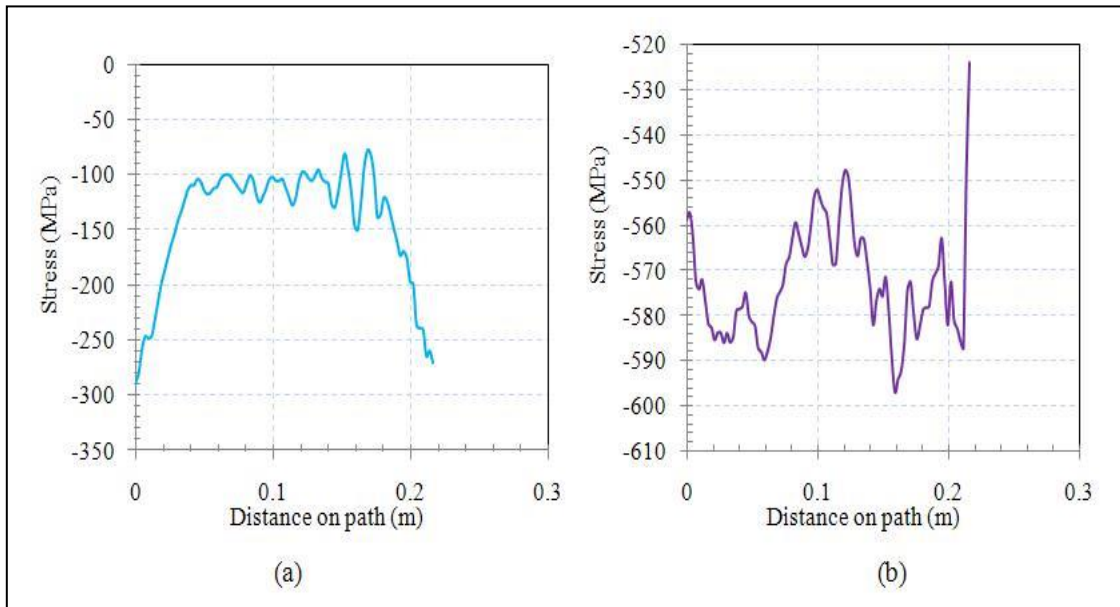


Figure10. Changes diagram of the (a) maximum and (b) minimum principal stress at the bottom surface of T-shape tube path

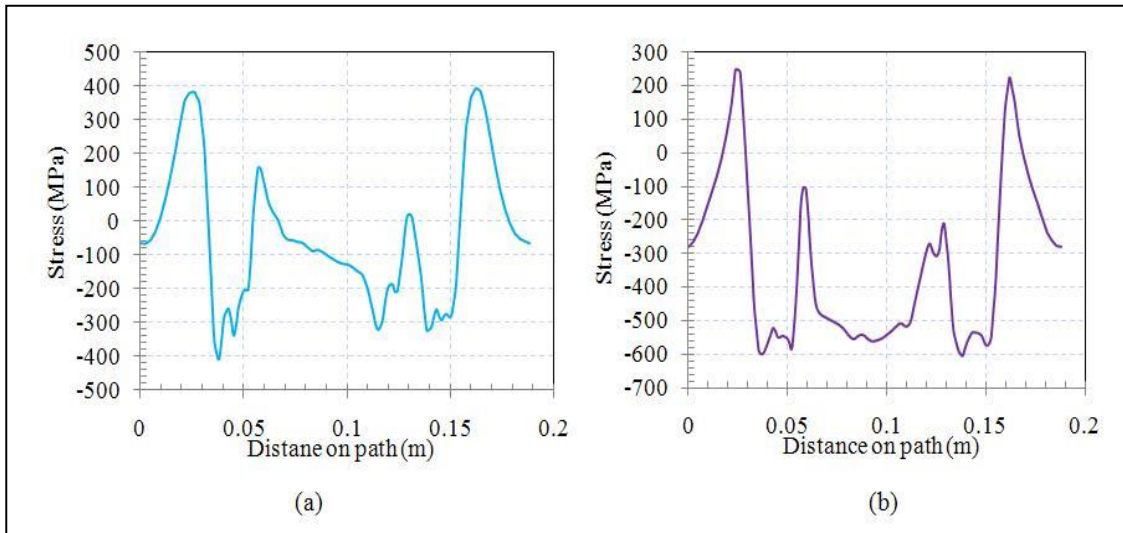


Figure 11. Changes diagram of the (a) Maximum and (b) Minimum principal stress at the transition annular path of the protrusion

Figure 12 exhibits the changes of the maximum and minimum principal stress along the depth path at the top of the protrusion. As can be seen, the maximum and minimum principal stress increases with increasing depth of the top of the protrusion.

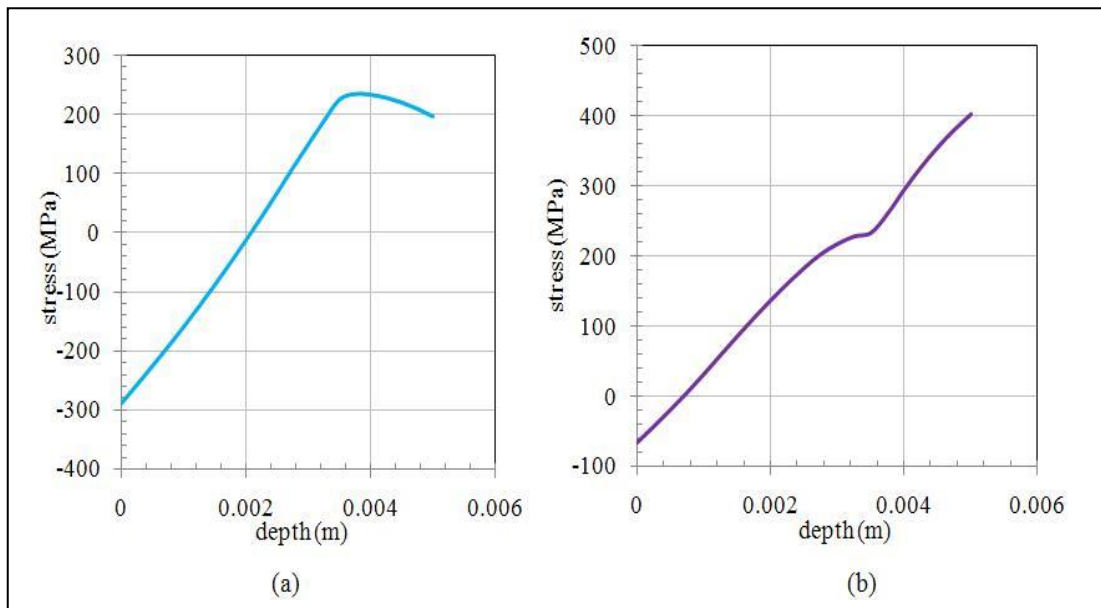


Figure 12. The maximum and minimum principal stress along the depth path at the top of the protrusion

4. Validation

The experimental test was carried out to confirm the validity of the FE results. For experimental measuring of residual stress, two hydroformed T-shape parts was selected. As regard of simulation results, the maximum residual stress is the top of the protrusion. So, the experiment set up was attached at the top of the protrusion as shown in Figure 3.

The comparison of hole drilling results and FE results was presented in Figure 13. As it can be seen from Figure 13 that the value of residual stress in experimental and simulation results were in good agreement. The maximum variation of FE results for minimum residual stress was 34.3% with case 1 and 22.91% with case 2. The maximum variation of FE results for maximum residual stress was 1% with case 1 and 27.31% with case 2.

The variation in the FE results may be due to various factors: (a) plasticity effect, (b) the effect of stress concentration, (c) error in measurement of the residual stress,(d) accuracy of finite element modeling.

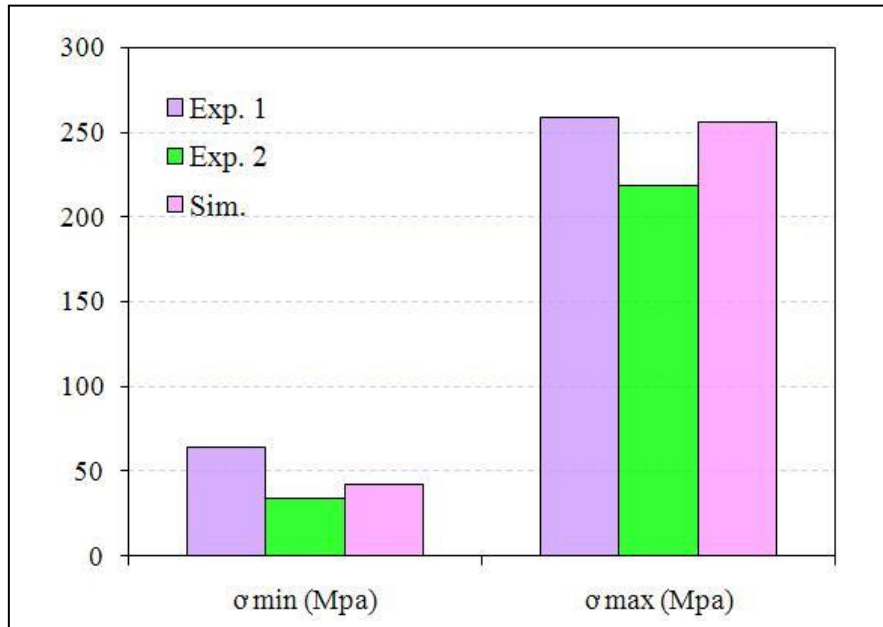


Figure13. The comparison of experimental and FE results

Figure 14 represents the axial cross section of hydroformed T-shape tube. The initial length of the steel tube was about 216 mm that reached to 126 mm after THF process. After hydroforming process, the final protrusion height of T-shape tube was measured. A large height of branch for hydroformed T-branch about 43.08 mm was obtained from an initial sample. The simulation results was shown that the maximum available height of branch is about 43.44 mm.0.8 % higher height obtained in simulated T-branch hydroforming process in comparison with the experimental T-branch hydroforming process.

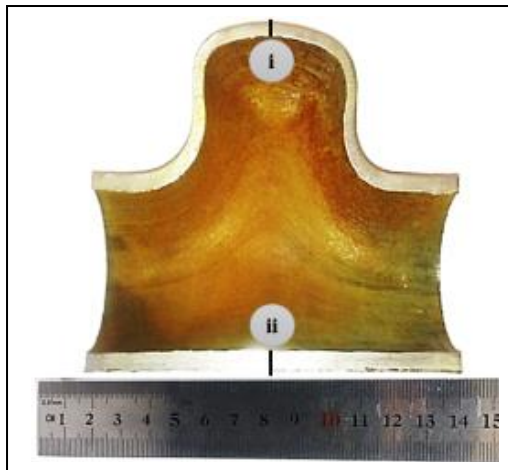


Figure14. Axial cross section of experimental T-branch sample

For measuring the thickness of hydroformed experimental tube, two positions were selected. Position “i” is the top of protrusion zone and position “ii” is the center of the lower surface of T-shape tube. These two positions are the critical zones in the contour of thickness distribution of simulated T-shape tube. Position “i” is a thickened point and position “ii” is a thinning point at the final part. The thickness of position “i” is 4.04 mm while the same point in the simulated part is 3.96 mm. The percentage deviation of simulation results with experimental results for the thickness of the protrusion wall is about 1.8%. The thickness of position “ii” is 6.54 mm while the same point in the simulated part is 6.75 mm. The maximum variation of lower wall thickness in FE results was 3.21%.

5. Conclusions

In this paper, an experimental study and FE simulation of T-branch tube hydroforming were performed. The distribution of thickness and residual stress was successfully simulated and the FE results were validated with experimental results. The following conclusions have been reached:

- The maximum principal stress in the middle of the piece has its own maximum value.
- The maximum value of minimum principal stress is located in the top of the protrusion and the fillet transition region of the protrusion.
- The values of residual stress in experimental and simulation results were in good agreement, in which the maximum variation of FE results for minimum residual stress was 34.3% for case 1 and 22.91% for case 2. The maximum variation of FE results for maximum residual stress was 1% for case 1 and 27.31% for case 2.
- The length of the processed steel tube was reduced from an initial value of 216 mm to 126 mm.
- After the hydroforming process, the height of the branch for the hydroformed T-branch was about 43.08 mm, obtained from an initial cylindrical tube, while the same value in simulation results is about 43.44 mm, with a 0.8% difference in experimental value.
- The thicknesses of the two selected positions in the hydroformed sample are 4.04 mm and 6.54 mm, while the same points in simulated parts are 3.96 mm and 6.75 mm, respectively. The percentage deviation of simulation results with experimental results are about 1.8% and 3.21%.

6. References

- [1] Islam, M. D., Olabi, A. G. and Hashmi, M. S. J. 2006. Feasibility of multi-layered tubular components forming by hydroforming and finite element simulation. *Journal of Materials processing technology*, 174, 394-398.
- [2] Devereaux Anthony, P., Gray John, E. and Parker William, M. 1940. Apparatus for making wrought metal t's, ed: Google Patents.
- [3] Limb, M., Chakrabarty, J., Garber, S. and Mellor, P. 1973. The forming of axisymmetric and asymmetric components from tube. In *Proceedings of the 14th International MTDR Conference*.
- [4] Woo, D. M. 1964. The analysis of axisymmetric forming of sheet metal and the hydrostatic bulging process. *International Journal of Mechanical Sciences*, 6, 303-317.
- [5] Thiruvardhelvan, S. 1994. A theory for the bulging of aluminium tubes using a urethane rod. *Journal of materials processing technology*, 41, 311-330.
- [6] Powell, G. and Avitzur, B. 1973. Forming of tubes by Hydraulic Pressure. In *Proceedings of the North American Metalworking Research Conference*.
- [7] Ueda, T. and Ogura, T. 1968. Liquid bulge forming. *Metalworking Prod*, 24, 73-81.
- [8] Koç, M. and Altan, T. 2001. An overall review of the tube hydroforming (THF) technology. *Journal of Materials Processing Technology*, 108, 384-393.
- [9] Hwang, Y. M., Lin, T. C. and Chang, W. C. 2007. Experiments on T-shape hydroforming with counter punch. *Journal of Materials Processing Technology*, 192, 243-248.
- [10] Hwang, Y. M. and Lin, Y. K. 2002. FE-simulations of T-shape tube hydroforming. ed: *Trans Tech Publ*, 233, 317-322.
- [11] Crapps, J., Marin, E. B., Horstemeyer, M. F., Yassar, R. and Wang, P. T. 2010. Internal state variable plasticity-damage modeling of the copper tee-shaped tube hydroforming process. *Journal of Materials Processing Technology*, 210, 1726-1737.
- [12] Manabe, K.-i., Suetake, M., Koyama, H. and Yang, M. 2006. Hydroforming process optimization of aluminum alloy tube using intelligent control technique. *International Journal of Machine Tools and Manufacture*, 46, 1207-1211.
- [13] Loh-Mousavi, M., Bakhshi-Jooybari, M., Mori, K. I. and Hyashi, K. 2008. Improvement of formability in T-shape hydroforming of tubes by pulsating pressure. *Proceedings of the Institution of Mechanical Engineers, Part B: Journal of Engineering Manufacture*, 222, 1139-1146.
- [14] Ray, P. and Mac Donald, B. J. 2005. Experimental study and finite element analysis of simple X- and T-branch tube hydroforming processes. *International Journal of Mechanical Sciences*, 47, 1498-1518.
- [15] Prime, M. B. 1999. Residual stress measurement by successive extension of a slot: the crack compliance method. *Applied Mechanics Reviews*, 52, 75-96.
- [16] Beaney, E. M. 1976. Accurate measurement of residual stress on any steel using the centre hole method. *Strain*, 12, 99-106.
- [17] Chen, J., Peng, Y. and Zhao, S. 2009. Comparison between grating rosette and strain gage rosette in hole-drilling combined systems. *Optics and Lasers in Engineering*, 47, 935-940.
- [18] Prime, M. B. 1997. Residual stress measurement by successive extension of a slot: a literature review. Los Alamos National Lab., NM (United States).

Numerical and Experimental Study of Residual Stress Measurement and Thickness Distribution ..., pp. 45-58

- [19] Astm, E. 2008. Standard Test Method for Determining Residual Stresses by the Hole Drilling Strain Gage method. ed: ASTM International Conshohocken, PA.
- [20] Giri, A., Pandey, C., Mahapatra, M. M., Sharma, K. and Singh, P. K. 2015. On the estimation of error in measuring the residual stress by strain gauge rosette. *Measurement*, 65, 41-49.
- [21] Totten, G., Howes, M. and Inoue, T. 2002. Handbook of residual stress and deformation of steel: ASM International. Materials Park, Ohio.